Effects of Clay Contents on the Dynamic Mechanical and Rheological Properties of Polypropylene/MAH-*g*-POE/Clay Composites

Xiuying Qiao,[1] Weixia Zhong,[1] Kang Sun,[1] Xiaodong Chen[2]

[1]*State Key Laboratory of Metal Matrix Composites, School of Materials Science and Engineering, Shanghai Jiao Tong University, Shanghai 200240, China*
[2]*Shanghai Sunny New Technology Development Co., Ltd., Shanghai 201109, China*

Received 3 December 2008; accepted 9 February 2009
DOI 10.1002/app.30218
Published online 24 June 2009 in Wiley InterScience (www.interscience.wiley.com).

ABSTRACT: A series of polypropylene/maleic anhydride grafted polypropylene octane elastomer (MAH-*g*-POE)/clay (PPMC) nanocomposites were prepared with a novel compatilizer MAH-*g*-POE and different contents of octadecyl amine modified montmorillonite, and the effects of clay contents on the dynamic mechanical and rheological properties of these PPMC composites were investigated. With clay content increasing, the characteristic X-ray diffraction peak changed from one to two with intensity decreasing, indicating the decreasing concentration of the intercalated clay layers. The gradual decrease of crystallization temperature of PPMC composites with the increase of clay loading should be attributed to the preferred intercalation of MAH-*g*-POE molecules into clay interlayer during blending, which is also reflected by scanning electron microscopy observations. By evaluating the activation energy for the glass transition process of MAH-*g*-POE and polypropylene (PP) in the PPMC composites, it is found that clay intercalation could cause the restriction effect on the glass transition of both MAH-*g*-POE and PP, and this restriction effect appears stronger for PP and attained the highest degree at 5 wt % clay loading. The melt elasticity of PP could be improved apparently by the addition of MAH-*g*-POE, and 5 wt % clay loading is enough for further enhancing the elastic proportion of PP. © 2009 Wiley Periodicals, Inc. J Appl Polym Sci 114: 1702–1709, 2009

Key words: poly(propylene); MAH-*g*-POE; clay; DMTA; rheology

INTRODUCTION

Polymer/clay nanocomposites have attracted much attention in the past years because of their significant improvement of physical properties with respect to their neat polymer and conventional composites.[1–3] Polypropylene/clay nanocomposite (PPCN), as one of the pioneer systems in the field of nanocomposites, has been extensively studied in a number of publications.[4–11] The properties of PPCNs are strongly affected by the intercalation and exfoliation of clay in polyproylene (PP) matrix. As described in the previous work,[12,13] the use of maleic anhydride grafted polypropylene (MAH-*g*-PP) is considered to be effective to compatibilize clay layers and PP molecules due to the hydrogen bonding between MAH groups of MAH-*g*-PP chains and hydroxyl groups attached on clay platelets. PPCNs compatibilized with MAH-*g*-PP display more homogeneous dispersion of clay layers accompanied with higher stiffness and modulus. However, an undesirable decrease of toughness appears in these composites and somewhat limits the practical application of these PPCNs.

A sort of polyethylene octane elastomer (POE), which was developed by using a metallocene catalyst by Dow and Exxon, has received much interests due to its narrow molecular weight and homogeneous octane distribution,[14] and MAH-*g*-POE has been used as a modifier to improve the compatibility of incompatible composites. The compatibilization of MAH-*g*-POE in PP-clay systems containing a fixed 5 wt % loading of clay was discussed and investigated in our previous work.[15] Studies showed that the use of MAH-*g*-POE as a compatibilizer could better the dispersion of clay layers in PP matrix, and the resultant nanocomposites exhibited both improved stiffness and toughness. Furthermore, MAH-*g*-POE was well miscible with the PP matrix, even with the concentration up to 20 wt %, in view of scanning electron microscopy (SEM) and dynamical mechanical thermal analyzer (DMTA) observations. However, the influence of clay contents has not been detected in PP/MAH-*g*-POE matrix yet; in this case, the effects of different clay loadings on the PP/MAH-*g*-POE/clay composites were extensively detected in this article.

DMTA is an important medium to measure the dynamic mechanical properties of materials. By

Correspondence to: K. Sun (ksun@sjtu.edu.cn).

means of DMTA, changes in the solid structure of a polymer after compounding with other materials could also be detected. The analysis of the storage modulus, loss modulus, and loss factor tan δ curves over a wide temperature and frequency range is useful for understanding the viscoelastic behavior and provides valuable insight into the relationship between the structure, morphology, and applicable properties of polymers and polymer composites.[16,17] The dynamical performance of various PP/MAH-*g*-PP/clay nanocomposites with different MAH-*g*-PP contents has been studied by DMTA in previous articles.

A good thermoforming material must have both viscous and elastic components at the forming temperature.[18] To understand the processibility of the final PP/clay composites, the rheological behavior of these materials in the molten state should be studied in detail. Understanding the rheological properties of nanocomposite melts is not only important in gaining a fundamental knowledge of the processibility but also helpful for understanding the structure–property relationships in these materials. Moreover, rheology potentially offers a method to assess the dispersion state of nanoclay in polymer/clay melts.[19,20]

In this article, novel PP/MAH-*g*-POE/clay (PPMC) nanocomposites were prepared by melt blending with different amounts of nanoclay. Effects of the clay loading on its dispersion within the PP/MAH-*g*-POE compounded matrix and the relationship between the structure, dynamic mechanical, and rheological properties were studied in details.

MATERIALS AND METHODS

Materials

The polymer matrix for the composites was PP homopolymer F401 (MFI = 2.5 g/10 min, $\rho = 0.91$ g/cm^3) produced by Sinopec Yangzi Petro Chemicals (Nanijing, China). The compatibilizer used was MAH-*g*-POE with 0.8% MAH content (POE Engage 8999, the product of DuPont Dow Elastomer, Wilmington, DE), provided by Shanghai Sunny New Technology Development (China). The organophilic clay was DK1, octadecyl amine modified montmorillonite, supplied by Zhejiang Fenghong Clay (Anji, China), as particles with an average size of 25 μm.

Preparation of PP/MAH-*g*-POE/clay composites

The PP/MAH-*g*-POE/clay nanocomposites were melt blended in a thermoplastic mixer of Rheocord 900 (HAAKE, Mess-Technic GmbH, Karlsruhe, Germany) by varying the clay content from 3 to 9 wt % with an increment of 2 wt %. The compositions and abbreviations of these nanocomposites were listed in Table I. The melt blending process was performed at 190°C with a rotor speed of 100 rpm for 15 min, and the obtained nanocomposites were compression-molded into pieces of 100 × 100 × 1 mm^3 for measurements.

TABLE I
Composition of the PPMC Composites

Sample	PP (wt %)	MAH-*g*-POE (wt %)	Clay (wt %)
PP	100	0	0
PPMC0	85	15	0
PPMC3	82	15	3
PPMC5	80	15	5
PPMC7	78	15	7
PPMC9	76	15	9

PPMC0–9: the numbers 0–9 represent the weight percent of clay loading.

Characterizations

The clay dispersion in different composites was studied at ambient temperature by using an X-ray diffractometer (XRD; D/MAXIII, Rigaku Corp., Tokyo, Japan), with a Cu Kα radiation ($\lambda = 0.154$ nm). All the samples were scanned by plates over a 2θ range of 1°–11° at a rate of 2°/min. When the XRD pattern exhibits a peak, it indicates that there exists a significant fraction of material with a regular stacked structure of clay layers. The basal spaces between the clay layers can be determined from the reflection peak in the XRD patterns by applying Bragg's diffraction law.

The phase structures of the composites were examined by a Hitachi-S-2150 scanning electron microscope (Hitachi Ltd., Tokyo, Japan) on the etched surfaces of cryogenically fractured specimens. All samples were etched in heptane (60°C) for 35 min to dissolve the compatilizer MAH-*g*-POE from the PP matrix and thus improving contrast between the phases. These samples were sputter-coated with gold-palladium alloy before viewing.

The thermal characteristics of the composites were analyzed on a differential scanning calorimeter (DSC) Q10 thermal analyzer (TA Instruments, New Castle, DE). Test specimens of 4–10 mg were first heated from 20 to 200°C at a rate of 20°C/min and then maintained there for 5 min to eliminate the effects of preconditions. In succession, the samples were cooled down to 20°C at a rate of 10°C/min (crystallizing cycle) and then heated again to 200°C at a rate of 10°C/min (melting cycle). From the thermograms, transition temperatures and enthalpies can be obtained.

The solid dynamic loss factor for different PP composites was studied on a dynamic mechanical thermal analyzer (DMTA IV; Rheometric Scientific Inc., Piscataway, NJ). Test samples were cut into bars (about 15 mm long, 4 mm wide) from the

compression-molded plaques. The experiments were performed in a single-point bending mode over a wide frequency range (0.1, 1, 5, and 10 Hz) with a temperature range from −100 to 150°C and a heating rate of 3°C/min under a controlled sinusoidal strain. The dynamic mechanical property parameters, such as the storage modulus (E'), loss modulus (E''), and loss factor (tan $\delta = E''/E'$), were recorded as a function of temperature. The values of activation energy of PP chain segments relaxation in different composites were calculated by the Arrhenius equation[21]:

$$f = f_0 \exp \frac{-\Delta E_a}{RT} \quad (1)$$

where f_0 is a frequency constant, R is the gas constant [8.314 J/(K mol)], f corresponds to different testing frequency during temperature sweep experiment, ΔE_a is the activation energy for this glass relaxation, and T is the peak temperature of this transition process. According to this equation, the slope of the straight line obtained from the plot of log$f$ versus $1/T$ is proportional to the activation energy, ΔE_a.

The thermoforming properties were investigated by using a strain-controlled rheometer (ARES Rheometer, Rheometric Scientific Inc., Piscataway, NJ), with 25-mm-diameter parallel plates. Low-amplitude oscillatory shear experiments were performed under ambient atmosphere over a frequency range of 0.01–100 rad/s at 190°C to study the linear viscoelasticity of samples including storage modulus G', loss modulus G'', and the loss factor tan $\delta = G''/G'$. Before testing, samples were annealed between the parallel plates for 5 min to ensure the stability and uniformity of the sample temperature.

RESULTS AND DISCUSSION

Clay dispersion

XRD patterns of clay and PPMC composites with different clay loading are presented in Figure 1. As shown in Figure 1, the virgin clay exhibits a single diffraction peak at about 3.6°, corresponding to an interlayer spacing (d-spacing) of 2.1 nm, and the formation of this kind of crystal lattice should result from the face-to-face stacking of the unit layers of montmorillonite. After clay is blended into the PP matrix compatibilized with MAH-g-POE, the clay dispersion varies with the increase of clay content in the PPMC composites. With 3 wt % clay loading, the PPMC3 nanocomposite displays a single weak and wide peak at about 2.7°, corresponding to a basal d-spacing of 3.3 nm. The great increase of the d-spacing of clay layers in PPMC3 indicates that 3 wt % loading clay could be well dispersed in the composite by the use of 15 wt % MAH-g-POE compatilizer

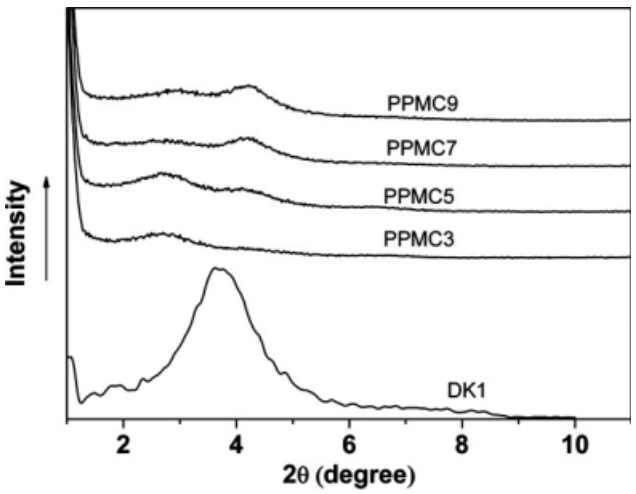

Figure 1 X-ray diffraction patterns of clay and PPMC composites.

during melt blending, and the clay layers have been intercalated with the expansion of the layer structure through the diffusion of the polymer chains into the silicate galleries. However, with the addition of 5 wt % clay, the PPMC5 shows two diffraction peaks, one stronger at 2.7° (Peak 1) originating from the intercalated clay layers and another weaker at 4.1° (Peak 2) originating from the stacked and unexpanded clay layers. With the further increase of clay loading, Peak 1 gradually shifts to higher angle location and decreases in intensity, while Peak 2 gradually becomes stronger, and such change tendency turns stable until the clay content increases to 9 wt %. These phenomena suggest that when the clay addition is above 5 wt % the clay dispersion substantially becomes poorer in PP/MAH-g-POE matrix; as a result, unexpanded stacks of clay layers appears more and more with the increase of clay loading from 5 to 7 and even to 9 wt %.

As is known,[22] the concentration of the intercalated clay layers with a given spacing is proportional to the area under the corresponding XRD peak, while the exfoliated structure of clay does not display any peak in its XRD pattern. On the basis of the above XRD patterns of the PPMC composites in Figure 1, the concentration of the intercalated and unexpanded clay layers corresponding to the characteristic peaks at about $2\theta = 2.7°$ (Peak 1, $d = 3.3$ nm) and $2\theta = 4.1°$ (Peak 2, $d = 2.1$ nm) could be respectively estimated according to the schematic in Figure 2, and the corresponding results were listed in Table II. As seen from Table II, it is more evident that with the increase of clay loading, the concentration of the unexpanded clay layers in PP/MAH-g-POE matrix increases, while the concentration of the intercalated clay layers decreases. Thus it can be seen that a small amount of clay loading can facilitate the intercalation of polymer molecules, but a large amount of clay

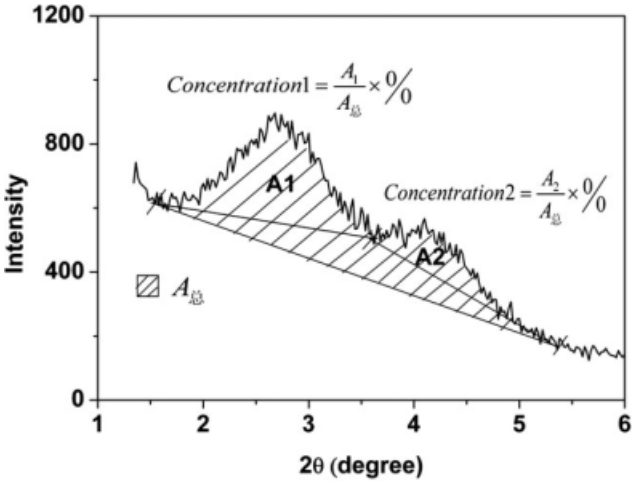

Figure 2 Estimation of the concentration of the intercalated and unexpanded clay layers in PPMC composites according to the characteristic X-ray diffraction peaks.

loading will make it difficult for the stacked clay layers to be expanded and will be disadvantageous for the good dispersion of clay layer in PP matrix.

Microstructure

SEM micrographs of the etched cryogenic fracture surfaces of PP and PPMC composites with different amounts of clay are shown in Figure 3. After being etched by heptane with the removal of the MAH-*g*-POE phase, the PP/MAH-*g*-POE (PPMC0) sample exhibits many well-dispersed 600- to 800-nm holes in the surface. For PP/MAH-*g*-POE/clay composites, the etched holes become gradually blurry as the clay addition increases from 3 to 5 wt % but appears distinct again with the clay loadings of 7 and 9 wt %. From these micrographs, it could be concluded that the clay layers could effectively block heptane to dissolve MAH-*g*-POE away from the surface of PP-based composites, due to the gradual bonding of MAH-*g*-POE molecules into the clay platelets. However, this block effect is somewhat weakened in PPMC9 because of the decreasing of the intercalated structure of clay layers in this composite.

Thermal analysis

Table III summarizes the DSC results of PP and PPMC composites including the values of onset crystallization temperature ($T_{c,\text{onset}}$), peak crystallization temperature ($T_{c,p}$), onset melting temperature ($T_{m,\text{onset}}$), peak melting temperature ($T_{m,p}$), normalized crystallization enthalpy ($\Delta H_c/\chi$), and normalized melting enthalpy ($\Delta H_m/\chi$), in which χ represents the total weight ratio of MAH-*g*-POE and clay in SF/PCL composites. As shown in Table III, it is clear that 15 wt % MAH-*g*-POE blended into PP matrix plays some nucleation role in PP crystallization, considering the increase of $T_{c,\text{onset}}$ and $T_{c,p}$ values. However, the corresponding PPMC0 composite has lower $T_{m,\text{onset}}$ and $T_{m,p}$ values than pure PP does, indicating of a lower degree of ordered structure. As the addition of clay increases from 3 to 7 wt %, the PPMC composites display a decreasing $T_{c,\text{onset}}$ and $T_{c,p}$, whereas the values of $T_{c,\text{onset}}$ and $T_{c,p}$ of PPMC9 with 9 wt % clay inversely appear a little increased. This phenomenon suggests that the nucleation role of MAH-*g*-POE on PP crystallization is gradually decreased as the clay content increases from 3 to 7 wt %, which should be attributed to the preferred intercalation role of MAH-*g*-POE molecules into clay interlayers during blending, in agreement with the SEM analysis. As seen from the data in Table III, $T_{m.\text{onset}}$ also slightly decreases in PPMC composites, similar to the variation of $T_{c,\text{onset}}$ and $T_{c,p}$ with clay loading increasing, whereas the value of $T_{m,p}$ distinctly decreases in PPMC9 composite. From this result, it could be assumed that the perfection degree of PP spherulites apparently decreases in PPMC9, which further confirms the poor clay dispersion in PPMC9. From Table III, it can also be found that the blending of MAH-*g*-POE into the PP matrix raises the thermal enthalpy of PP to a certain degree, especially the melting enthalpy, while the addition of clay further strengthens this effect. It is known that small amounts of clay can effect as nucleator to enhance the crystallization of polymer materials. However, for our PPMC composite system, due to the interaction of clay layers with the MAH-*g*-POE molecules, the addition of clay does not accelerate the crystallization process of PP obviously but merely increases the crystallinity of PP to a certain degree.

Dynamic mechanical properties

The loss factor (tan δ) curves of PP, MAH-*g*-POE, and PP/MAH-*g*-POE (PPMC0) as a function of temperature at 1 Hz are depicted in Figure 4. As shown in Figure 4, the pure PP exhibits only one resolved

TABLE II
Concentration of Intercalated and Unexpanded Clay Layers in PPMC Composites Estimated from the Corresponding X-ray Diffraction Peak Area

	Peak 1		Peak 2	
Sample	2θ (°)	Concentration of intercalated clay layers (%)	2θ (°)	Concentration of unexpanded clay layers (%)
PPMC3	2.7	93.1	–	–
PPMC5	2.7	44.9	4.1	10.0
PPMC7	2.7	18.8	4.2	35.0
PPMC9	2.9	9.4	4.2	33.5

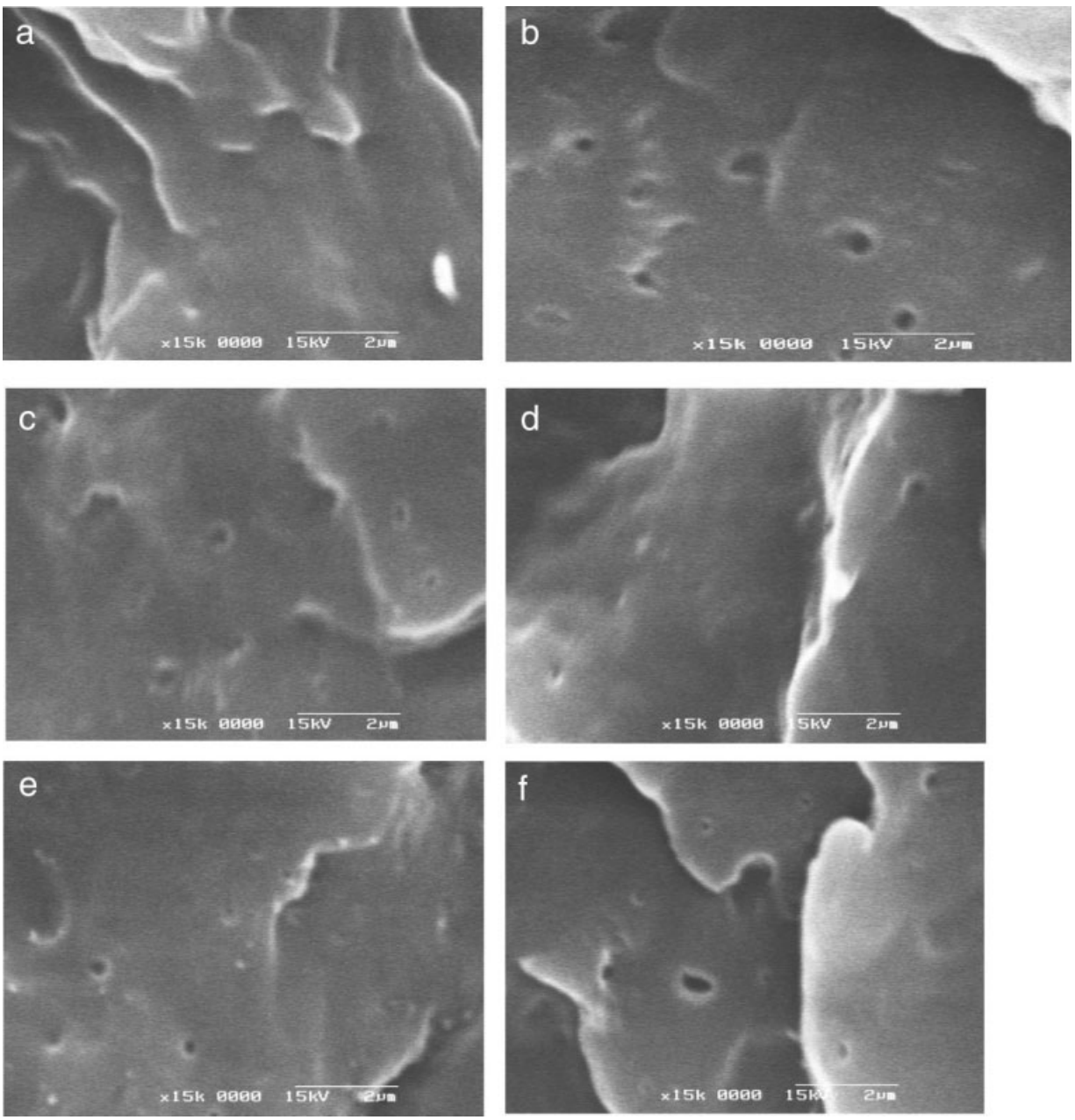

Figure 3 Cryogenic fractured and etched surfaces of PP and PPMC composites: (a) PP; (b) PPMC0; (c) PPMC3; (d) PPMC5; (e) PPMC7; (f) PPMC9.

peak at 11.3°C, associated with the glass transition of PP in amorphous phase. The tan δ curve of MAH-*g*-POE displays a sharp relaxation peak at −22.1°C, corresponding to the glass transition process of MAH-*g*-POE. For the PP/MAH-*g*-POE composite, the tan δ curve shows two relaxation peaks, one located at −38.1°C and another at 10.5°C. The great shift of the glass transition peak of MAH-*g*-POE from −22.1 to −38.1°C implies that the polar interactions among MAH-*g*-POE molecules are considerably reduced by the interference from nonpolar PP molecules, which agrees with the well-dispersed holes of MAH-*g*-POE in SEM micrographs. To investigate the effects of clay addition on the changes of the glass transition processes of MAH-*g*-POE and PP in solid PPMC composites in detail, the segmental tan δ curves of MAH-*g*-POE and PP in PPMC composites are respectively discussed in Figure 5. Furthermore, the corresponding values of activation energy for the glass transition processes of MAH-*g*-POE and PP in different PPMC composites are shown in Table IV.

As seen in Figure 5(a), the tan δ curves for different PPMC composites display a clear peak at about −38°C to −34°C, corresponding to the glass relaxation of MAH-*g*-POE. As compared with PPMC0,

TABLE III
DSC Results of PP and PPMC Composites

Sample	$T_{c,\text{onset}}$ (°C)	$T_{c,p}$ (°C)	$T_{m,\text{onset}}$ (°C)	$T_{m,p}$ (°C)	$\Delta H_c/\chi$ (J/g)	$\Delta H_m/\chi$ (J/g)
PP	117.1	111.9	157.5	167.0	97.0	91.8
PPMC0	120.1	113.9	156.8	166.9	97.5	93.5
PPMC3	119.1	112.3	156.9	166.8	96.1	95.4
PPMC5	118.7	112.8	156.3	166.8	100.3	98.5
PPMC7	116.8	110.7	155.8	168.9	97.1	92.4
PPMC9	118.9	113.9	157.0	165.4	104.6	105.8

with the variation of clay addition, the peak temperature for PPMC composites slightly increases as the clay addition increases from 3 to 5 wt % and then decreases when the clay content further increases, but the peak shape hardly changes. The activation energy for this process exhibits similar variation tendency, just as seen in Table IV, which suggests that less than 5 wt % addition of clay could somewhat interfere with the glass transition of MAH-*g*-POE due to the intercalation of MAH-*g*-POE molecules into clay layers, whereas the clay loadings of 7 and 9 wt % inversely facilitate this transition as regards the lower values of activation energy of PPMC7 and PPMC9 than that of PPMC0. These phenomena are in agreement with the results of the SEM micrographs. In addition, the good low-temperature toughness endowed by MAH-*g*-POE in PPMC composites are still retained even at high clay loading of 9 wt %.

In Figure 5(b), the tan δ curve exhibits a relaxation peak at 10–12°C, corresponding to the glass transition of PP in different PPMC composites. The peak temperature slightly shifts to a higher value for PPMC5 than for other PPMC composites, but the value of the activation energy (seen in Table IV) appears greatest for PPMC5, which implies that the activation energy is more sensitive to the clay content than the glass transition temperature for PP in PPMC composites. Blending of clay into PP matrix would cause restrictions on the glass transition of PP, and this restriction attains a higher degree at 5 wt % than at 7 or 9 wt % loading, primarily correlated with the clay layers dispersion within its composite. From the above discussion, it could be concluded that the blending of clay layers into the PP/MAH-*g*-POE matrix has a stronger effect on the glass transition of PP than that of MAH-*g*-POE, and 5 wt % loading of clay layers is enough for this

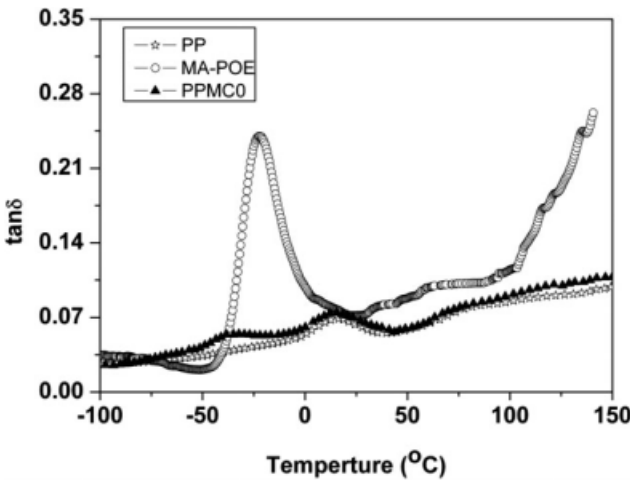

Figure 4 The loss factor (tan δ) of PP, MAH-*g*-POE, and PPMC0 as a function of temperature at 1 Hz.

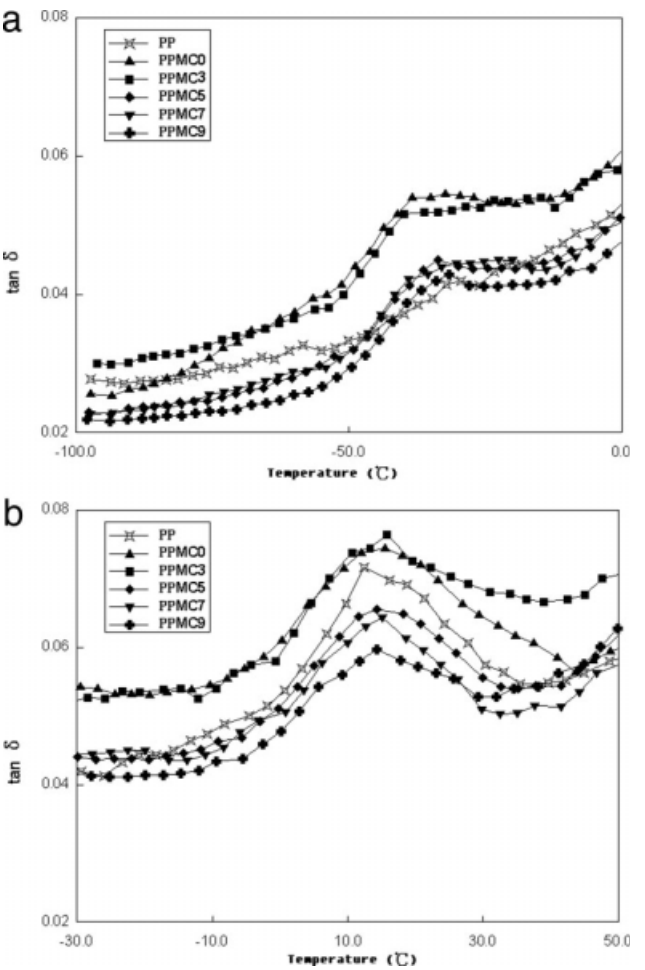

Figure 5 Variations on the tan δ curves of MAH-*g*-POE and PP in PPMC composites with different clay loadings: (a) MAH-*g*-POE; (b) PP.

TABLE IV
Values of the Glass Transition Temperature and Activation Energy of PP and PPMC Composites

Sample	$T_{g'PP}$ (°C)	$T_{g'MAH\text{-}g\text{-}POE}$ (°C)	$\Delta E_{a'PP}$ (kJ/mol)	$\Delta E_{a'MAH\text{-}g\text{-}POE}$ (kJ/mol)
PP	11.3	—	607.1	—
PPMC0	10.5	−38.4	356.4	267.5
PPMC3	11.2	−37.2	422.9	242.8
PPMC5	12.0	−34.3	540.5	275.0
PPMC7	11.3	−35.1	449.3	218.9
PPMC9	10.6	−35.4	401.9	180.5

system in view of the amount and dispersion improvement.

Linear viscoelastic properties

The melt shear viscosity (η*), storage modulus (*G*′), loss modulus (*G*″), and loss factor (tan δ) of PP and PPMC composites as a function of frequency (ω) at 190°C are shown respectively in Figure 6(a–d). Blending of 15 wt % MAH-*g*-POE into the PP matrix causes stronger sensitivity of η* versus ω, higher shear modulus (*G*′ and *G*″) at low frequency, as well as lower tan δ for the resultant PPMC0 melt than for the pure PP. This result shows that the melt elasticity of PP could be improved apparently by the addition of MAH-*g*-POE. With 3 wt % clay loadings in the PP/MAH-*g*-POE matrix, the PPMC3, although displaying a reduced η*, *G*′, and *G*″ at the frequency range of 10^{-1}–10^{2} rad/s shows a solid-like response as regards the pronounced *G*′–ω platform at low frequency of 10^{-2}–10^{0} rad/s. The loss factor (tan δ) of PPMC3 slightly decreases especially at low frequency. This phenomenon shows that small loading of 3 wt % clay could enhance the elastic proportion of the corresponding melt, and this elastic enhancement is further strengthened by increasing the clay content to 5 wt %. However, after increasing the clay loading up to 7 or 9 wt %, the PPMC7 or PPMC9 melt

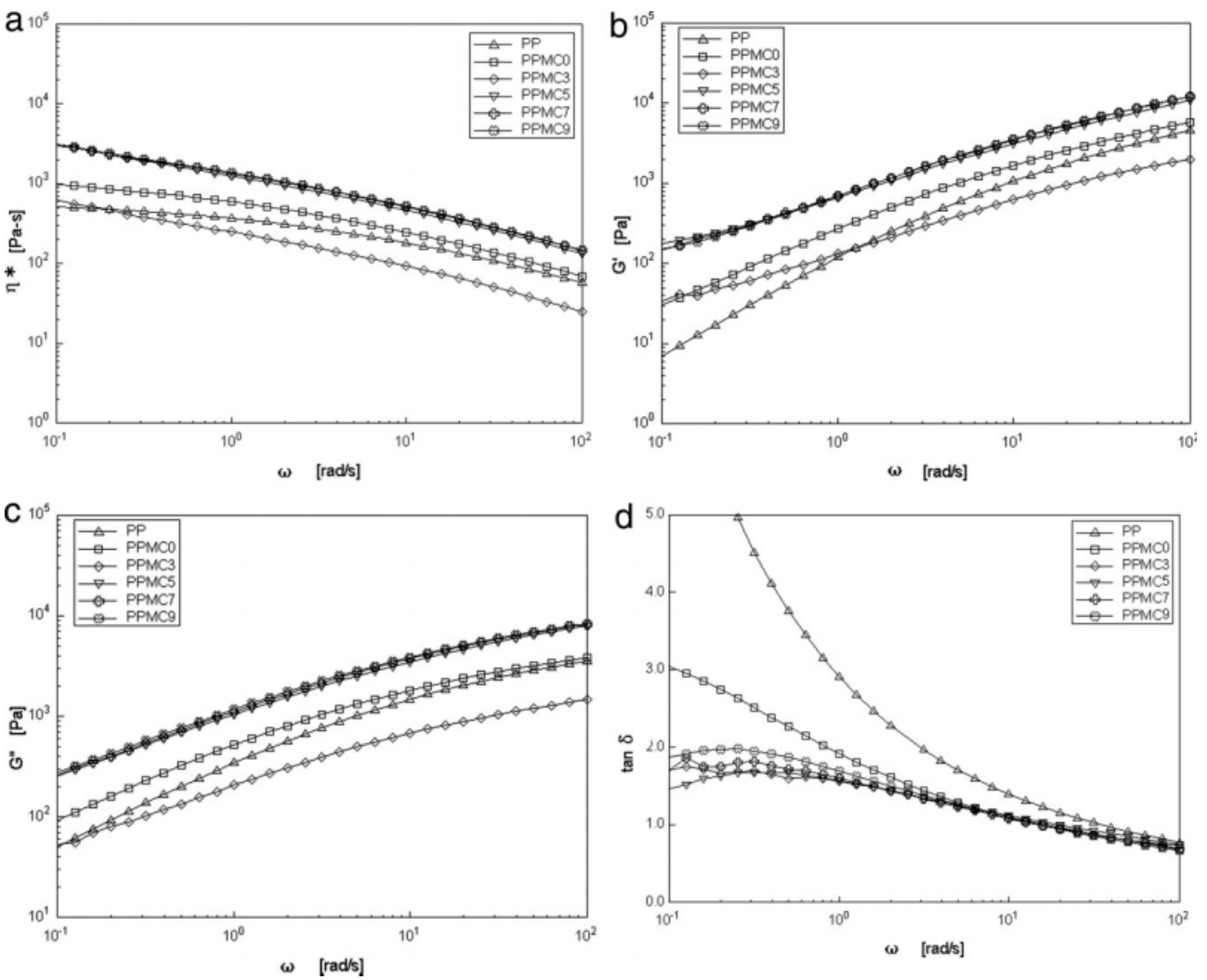

Figure 6 Rheological behaviors of PP and PPMC composites at 190°C: (a) melt viscosity versus frequency; (b) storage modulus versus frequency; (c) loss modulus versus frequency; (d) loss factor versus frequency.

displays almost the same linear viscoelastic behavior as PPMC5 does. This rheological result could further confirm that 5 wt % clay loading is enough for the PP/MAH-*g*-POE matrix, and it is also an optimum loading to enhance the elastic proportion of PP.

CONCLUSIONS

By melt blending method, a series of PPMC nanocomposites were prepared with different clay contents and a fixed content of MAH-*g*-POE as a novel compatilizer. Through the measurements of XRD, SEM, DSC, DMTA, and rheological property, the influences of clay layer dispersion on the dynamic mechanical and rheological behaviors of these kinds of hybrid materials were investigated.

According to the XRD results, when the clay addition is above 5 wt %, the clay dispersion becomes poorer in PP/MAH-*g*-POE matrix with the decrease of the concentration of the intercalated clay layers, which indicates that small amount of clay loading can facilitate the intercalation of polymer molecules and good dispersion of clay layer in PP matrix, just as reflected by the SEM observations. The intercalation of MAH-*g*-POE molecule into clay interlayers will result in a slight decrease of crystallization temperature and melting temperature. The addition of clay interferes with the glass transition process of both MAH-*g*-POE and PP in PPMC composites, and this restriction effect appears stronger for PP and attains the highest degree at 5 wt % clay loading. The melt elasticity of PP could be improved apparently by the addition of MAH-*g*-POE, and this elastic enhancement is further strengthened by the addition of clay until the amount of 5 wt %.

The authors thank Instrumental Analysis Center of Shanghai Jiao Tong University for the assistance with the measurements.

References

1. Svoboda, P.; Zeng, C. C.; Wang, H.; Lee, L. J.; Tomasko, D. L. J Appl Polym Sci 2002, 85, 1562.
2. Kawasumi, M.; Hasegawa, N.; Kato, M.; Usuki, A.; Okada, A. Macromolecules 1997, 30, 6333.
3. Hasegawa, N.; Okamoto, H.; Kato, M.; Usuki, A. J Appl Polym Sci 2000, 78, 1918.
4. Kurokawa, Y.; Yasuda, H.; Oya, A. J Mater Sci Lett 1996, 15, 1481.
5. Ding, C.; Jia, D. M.; He, H.; Guo, B. C.; Hong, H. Q. Polym Test 2005, 24, 94.
6. Manias, E.; Touny, A.; Wu, L.; Strawhecker, K.; Lu, B.; Chung, T. C. Chem Mater 2001, 13, 3516.
7. Leuteritz, B. A.; Pospiech, D.; Kretzschmar, B.; Willeke, M.; Jehnichen, D.; Jentzsch, U.; Grundke, K.; Janke, A. Adv Eng Mater 2003, 5, 678.
8. García-López, D.; Picazo, O.; Merino, J. C.; Pastor, J. M. Eur Polym J 2003, 39, 945.
9. Koo, C. M.; Kim, J. H.; Wang, K. H.; Chung, I. J. J Polym Sci Part B: Polym Phys 2005, 43, 158.
10. Reichert, P.; Nitz, H.; Klinle, S. Macromol Mater Eng 2000, 275, 8.
11. Chiu, F. C.; Lai, S. M.; Chen, J. W.; Chu, P. H. J Polym Sci Part B: Polym Phys 2004, 42, 4139.
12. Maiti, P.; Nam, P. H.; Okamoto, M.; Hasegawa, N.; Usuki, A. Mcromolecules 2002, 35, 2042.
13. Nam, P. H.; Maiti, P.; Okamoto, M.; Kotaka, T.; Hasegawa, N.; Usuki, A. Polymer 2001, 42, 9633.
14. Hwang, Y. C.; Chum, S.; Sehanobish, K. ANTEC 1994, 94, 3414.
15. Zhong, W. X.; Qiao, X. Y.; Sun, K.; Zhang, G. D.; Chen, X. D. J Appl Polym Sci 2006, 99, 2558.
16. Ward, I. M. Mechanical Properties of Solid Polymers; Wiley Interscience: London, 1971.
17. Amash, A.; Zugenmaier, P. J Appl Polym Sci 1997, 63, 1143.
18. Macauley, N.; Harkin-Jones, E.; Marphy, W. R. Plast Eng 1996, 52, 33.
19. Lele, A.; Mackley, M.; Galgali, G.; Ramesh, C. Prog Polym Sci 2003, 28, 1636.
20. Sinha Ray, S.; Okamoto, M. J Rheol 2002, 46, 1091.
21. Heijboar, J. Molecular Basis of Transitions and Relaxations; Meier, D. J., Ed.; Gordon and Breach Science Publishers: New York, 1978; p 75.
22. Ishida, H.; Campbell, S.; Blackwell, J. Chem Mater 2000, 12, 1260.